Author Version of : Estuarine, Coastal and Shelf Science, vol.250; 2021; Article no: 107149

Implications of micro-plankton and micro-detritus on the food web in the largest monsoonal estuary along the west coast of India

Karnan, C., *Jyothibabu, R., Arunpandi, N., Albin Jose., Parthasarathi, S.
CSIR-National Institute of Oceanography, Regional Centre, Kochi, India
*Corresponding author. Telephone: +91 484 2390814; Fax: +91 484 2390618
*E-mail address: rjyothibabu@nio.org

Abstract

This study presents how seasonal hydrographical changes affect the size structure of the micro-plankton community and thereby the availability of micro-detritus in the Kochi backwaters (KBW). Advanced quantification of plankton and detritus has been conducted using a FlowCAM, and we tested here the hypothesis that floodwater considerably increases the detritus availability in the KBW. Fortnightly time-series sampling was carried out over a year (2013-14) in a downstream location of the KBW. The water column in the study region was moderately rich in nutrients throughout the year (NO_3: > 1.4 µM; PO_4: > 0.3 µM; SiO_4: > 3 µM), showing the maximum levels during the Southwest Monsoon (SWM; June to September) followed by the Northeast Monsoon (NEM; November to February) and the Pre-Southwest Monsoon (PSWM; March-May). Following the above, the abundance and biomass of micro-autotrophs increased from the SWM (av. 1827 ± 1056 L^{-1} and av. 8 ± 2.53 µgC L^{-1}) and peaked during the PSWM (av. 23963 ± 17142 L^{-1} and av. 16 ± 9.49 µgC L^{-1}, respectively). The micro-heterotrophs (mean size and abundance) also remained high during the PSWM, followed by NEM. However, the micro-autotroph mean size was minimum during the PSWM (av. 20883 ± 2239 µm³), which increased during the SWM (av. 43510 ± 3611 µm³) and NEM (av. 35245 ± 8655 µm³). The micro-detritus was found highly abundant during both the PSWM and the NEM following the temporal trend in the abundance and biomass of micro-autotrophs and micro-heterotrophs in the study region, suggesting the active transfer of energy to the next trophic levels through smaller plankton as well as detritus. Also, the positive interrelationship of these components indicates that the primary source of micro-detritus is the dead plankton materials, which is an apparent deviation from the traditional belief that KBW possibly gets loaded with more detritus during the SWM due to the floodwaters.

Keywords: Micro-plankton; size structure; micro-detritus; monsoonal estuary, Kochi backwaters; FlowCAM

1. Introduction

Tropical estuaries usually sustain high biological production due to sufficient availability of nutrients and solar radiation. Being the most extensive estuarine system along the southwest coast of India, the hydrography of KBW is dominated by the high salinity water mass from the adjacent coastal Arabian Sea during non-monsoon/dry period (November to May) and with fresh water during the Southwest/Summer Monsoon (June to September). During the SWM, the western part of the Indian peninsula receives the highest seasonal rainfall due to strong south-westerly winds propelling rain clouds towards the region. In this season, large quantities of fresh water, along with high load of nutrients and suspended sediments, are introduced into the KBW through six rivers - Periyar, Muvattupuzha, Meenachil, Manimala, Pamba and Achancovil (Figure 1). The consistently high levels of nutrients in the KBW are mainly due to inputs from domestic, industrial, and agricultural sources (Balachandran et al., 2003; Jyothibabu et al., 2006; Madhu et al., 2007). The agrarian runoff from the vast paddy fields in the south and industrial effluent from establishments in the north are the significant sources of nutrients into the KBW (Balachandran et al., 2005; Madhu et al., 2007; Jose et al., 2011). During the SWM, coastal upwelling also brings nutrient-rich waters into the estuary through navigation channels (Ramamirtham and Jayaraman, 1963; Menon et al., 2000; Martin et al., 2010). KBW has mixed semidiurnal tides (~1 m), facilitating the intrusion of seawater up to the southern upstream (Thannermukkom Bund), ~40 km from the Kochi inlet. Previous studies have shown that a large amount of primary food remain unutilized in the KBW during the SWM due to the reduction in the abundance of significant consumers such as micro-zooplankton and mesozooplankton (Joseph and Kurup, 1989; Jyothibabu et al., 2006).

Changes in physical characteristics and nutrient distribution can affect the biological productivity of an estuary, especially the size and composition of plankton that is influenced by salinity (Qasim et al., 1972; Menon et al., 2000; Jyothibabu et al., 2006; Madhu et al., 2007). It was observed earlier that even though the KBW sustains reasonably high nutrient levels throughout the year, the primary production peaks only during the PSWM (Madhu et al., 2010; Sooria et al., 2015). Since most of the earlier studies were focused on plankton diversity and productivity, there is a lack of information about the microplankton size structure and its seasonality in the study region (Madhu et al., 2010). Studies have presented the seasonality of suspended particulate matter in different Indian estuaries, and most of them showed its high concentration associated with heavy rainfall and river runoff, especially during the SWM (Table 1). Past studies showed that suspended particulate matter increased with increased floodwater (Table 1), but the organic detritus in the settled material increased during the PSWM (Qasim and Sankaranarayanan, 1972).

Based on the above, a study was proposed to generate high-resolution seasonal data of microplankton (auto- and heterotrophic), micro-detritus, and the associated environmental setting in the downstream region of the KBW. Size estimation studies of plankton have aquired significant technical advancement in recent decades (Davis et al., 2004; Sosik and Olson, 2007; Alvarez et al., 2011; Karnan et al., 2017a). Here, we used FlowCAM, an automated image-based particle counting, and sizing instrument, to analyze the size structure of microplankton and micro-detritus. The objectives of the present study were to (a) quantify the micro-plankton size structure (both autotrophic and heterotrophic) and biomass distribution, (b) understand the seasonality of micro-detritus distribution and (c) explain how micro-plankton size structure and micro-detritus abundance influence the structuring of the plankton food web in the KBW.

2. Materials and methods

2.1. Sampling

Fortnightly time-series sampling was carried out at a fixed location near Bolghatty Island in the downstream region of the Kochi backwaters for a year (June 2013 - May 2014) (Figure 1). The sampling location was set at ~3 km away from the bar-mouth to avoid the recurrent influence of the waves; however, the selected site could still represent the significant hydrographical transformations in the downstream of the KBW adequately. The temperature, salinity, and Photosynthetically Available Radiation (PAR) were recorded using a portable CTD (Seabird Electronics, USA) and a handheld multi-parameter tester (Eutech Model TN 100). The turbidity was measured using a turbidity meter (Eutech). The water samples were collected for nutrient analysis and plankton quantification from a 5 L Niskin sampler. Major nutrients such as nitrate (NO_3), phosphate (PO_4), and silicate (SiO_4) were analyzed based on standard protocols (Grasshoff et al., 1983). Sub-samples of 0.2 - 1 L water was passed through a 300 µm nylon mesh to avoid large predators and stored in dark polythene bottles. The samples were concentrated by the siphoning method using a 20 µm nylon mesh cloth attached at one end of the tubing, details of which have been presented in Jyothibabu et al., (2006), and analyzed through a portable FlowCAM (Visual Spreadsheet IV; Sl. No. 614; Karnan et al., 2017a). In this study, we quantified only large-sized plankton and detritus components (>20 µm), excluding the smaller (<20 µm) components. Hourly rainfall data obtained from an online database (TRMM; Figure 2a), encompassing the KBW and its river catchment area, were analyzed on a fortnightly basis to understand the rainfall pattern during the present study period.

2.2. FlowCAM analysis

The recommended procedures by the Fluid Imaging Technologies were followed to prepare and analyze the plankton samples in FlowCAM (VS-IV; FlowCAM manual, 2009). The uniform settings in hardware and software of the FlowCAM were maintained throughout the sample analysis period to neutralize instrument-based technical errors. The volume of water samples collected for FlowCAM analysis, which varied periodically according to the particle concentration in the water. Typically, 200 ml - 1 L of fresh, pre-filtered, and concentrated water samples were passed through a 300 µm Field of View (FOV) flow chamber with the combination of a 4X objective lens, which gave 40 times magnified images in the FlowCAM analysis. The entire sample flow area in the flow chamber (FOV) was covered by the camera view so that all the particles were imaged. The concentration of particles in the water samples was maintained to an optimum level by choosing different final volumes of samples (10-50 ml). This ensured an almost single-line flow of particles in the flow chamber, rendering it more suitable for the laser mode of analysis (image capturing based on fluorescence and light scatter). A continuous flow of water sample through the flow chamber was ensured by running an external syringe pump (C71). The laser trigger mode (green laser; 532 nm) was used for the live samples, which also records the fluorescence properties of the particles. The plankton sample in the injecting funnel was regularly stirred up with a micropipette, aiding uniform frequency of the particle flow (Karnan et al., 2017a).

Images of interest were classified by deleting repetitive photographs and those of air bubbles. The detritus and organisms (genus level; Tomas et al., 1996) were initially classified by applying the statistical filter 'Like Selected Particles' algorithm available in the FlowCAM visual spreadsheet software. The above filter selects and sorts of particle images based on the statistical similarity of manually selected particles (n>2). All the unclassified images from the view window were classified manually. Finally, images of each class were visually inspected to avoid misclassification. The recommended combinations of setup (4X objective lens and 300 µm flow chamber) allowed us to classify most of the images up to the genus-level (Tomas et al., 1996). In contrast, some of the ambiguous images (smaller plankton components) were commonly grouped as autotrophs and heterotrophs. The damaged and partially decomposed plankton materials were included in the total detritus abundance. The micro-plastic particles were excluded by visual identification from the FlowCAM image list (Loder and Gerdts, 2015; Crawford and Quinn, 2017).

The biomass of individual plankton was estimated from the Area Based Diameter (ABD) volume as it includes long filaments, hooks, setae, and other protruded body parts during biovolume estimation (Karnan et al., 2017b). Based on the conversion factors available in standard literature

(Verity and Langdon, 1984; Verity et al., 1992; Michaels et al., 1995; Menden-Deuer and Lessard, 2000; Tada et al., 2000; Gowing et al., 2003; Marquis et al., 2011), the biovolumes (μm^3) were converted to carbon biomasses (µgC). Based on the aspect ratio of particles from the FlowCAM, the shape of the particles was estimated. The aspect ratio ranges from 0 to 1, in which 0 or its nearest values indicate needle-shaped particles, 1 or its most adjacent values indicate spherical-shaped particles and the mid-value 0.5 indicates elliptical-shaped particles (Olson, 2011a,b; Alvarez et al., 2012; Caromel et al., 2014; Karp-Boss and Boss, 2016).

2.3. Statistical tests

As per the central limit theorem, a larger sample size (n>30) may follow normal distribution while a smaller sample size must be tested for normality. In the present study, the sample size was small (n=24). Hence, we conducted the Shapiro-Wilk normality test along with Q-Q plotting (both in R-Studio software) for each biological parameter to assess their data distribution. For multi-seasonal comparison (among all groups), one way ANOVA (normal) and Kruskal-Wallis (non-normal) tests were carried out followed by Tukey's HSD and Dunn's post hoc tests (in R-Studio). For inter-seasonal comparison (between 2 groups), T-test (normal) and Wilcoxon test (non-normal) were carried out (in R-Studio). Selected multivariate statistical analysis tests were used to generalize the observations and draw meaningful conclusions from the environmental and biological data collected during the study. The redundancy analysis (RDA), along with Pearson's correlation matrix, is a useful method to understand the relationships among variables collated from different locations/periods. RDA analysis results are presented in a triplot, which offers variables as vectors and sampling periods as points. The vectors of different variables start from a centre point of a square plane (correlation score=0) and those stretched in different directions represent their relationship with other variables. The sampling points get dispersed among these vectors correspondingly, and the correlogram (a graphical representation of Pearson's correlation matrix) provides the coefficients. The RDA triplot was created in CANOCO 4.5 (Leps and Smilauer, 2003), and the correlogram was plotted with the correlogram package in R-Studio (Friendly, 2002; R Core Team, 2013).

3. Results

3.1. Hydrography

The rainfall data (Figure 2a) shows the mean precipitation in the region over the present study period. It may be observed that the rainfall was the highest (0.5 - 2 mm h^{-1}) during June-July (SWM), which decreased subsequently to <0.5 mm h^{-1} during the remaining period. The rainfall significantly

dropped in the catchment area (av. 0.09 ± 0.002 mm h^{-1}) during the NEM and later during PSWM (av. 0.14 ± 0.003 mm h^{-1}) (Table 2). As a consequence, the salinity was minimum during SWM (av. 1.2 ± 0.8 PSU), which increased during the NEM (av. 14.4 ± 2.5 PSU) and the PSWM (av. 11.7 ± 1.8 PSU; Figure 2a). The seasonal mean PAR was at a minimum during the SWM (av. 385 ± 22 µE m^{-2} s^{-1}) as compared to the NEM (av. 464 ± 9 µE m^{-2} s^{-1}) and PSWM (av. 520 ± 21 µE m^{-2} s^{-1}; Table 2).

3.2. Nutrients

All the nutrients remained high in the study region during the entire study period (Figure 2b). The nitrate concentration in the surface was always >1.4 µM, peaking during the SWM (av. 24 ± 3.2 µM L^{-1}), followed by the NEM (av. 6 ± 0.95 µM L^{-1}) and PSWM (av. 4 ± 0.87 µM L^{-1}). The silicate was also significantly higher during SWM (av. 74 ± 10.9 µM L^{-1}) and lowest during the NEM (15 ± 4.18 µM L^{-1}). The concentration of phosphate was maximum during the SWM (av. 2.09 ± 0.27 µm L^{-1}) and PSWM (av. 2.09 ± 0.21 µM L^{-1}), as compared to the NEM (av. 1.15 ± 0.21 µM L^{-1}; Table 2 and Figure 2b).

3.3. Biological parameters

3.3.1. Autotrophic micro-plankton

The abundance and biomass of microautotrophs were lower during the SWM and NEM as compared to the PSWM (Table 2; Figure 3). The variation in seasonal abundance was quasi-significant (Kruskal-Wallis, $p<0.1$) and the biomass were significant (Kruskal-Wallis, $p<0.05$). The abundance of autotrophic microplankton was lower during SWM (av. 1827 ± 1056 L^{-1}), lowest during NEM (av. 1254 ± 679 L^{-1}) and the highest during the PSWM (av. 23963 ± 17142 L^{-1}). The biomass of micro-autotrophs also followed the abundance pattern, as in during SWM it was low (av. 8 ± 2.53 µgC L^{-1}) and much lower during the NEM (av. 1 ± 0.44 µgC L^{-1}) compared to the PSWM (av. 16 ± 9.49 µgC L^{-1}) (Table 2). The variance in autotrophic biovolume/size among the seasons was not significant (ANOVA, $p>0.1$). The mean size of individual plankton showed a different trend with relatively large-sized autotrophic plankton individuals during SWM (av. 43510 ± 3611 μm^3) and NEM (av. 35245 ± 8655 μm^3) as compared to the PSWM (av. 20883 ± 2239 μm^3). Throughout the year, *Skeletonema* sp. was the most dominant micro-autotroph species in the study region, with *Eunotia* sp. being second-most dominant during the SWM, *Pleurosigma* sp. during the NEM and *Nitzschia* sp. during the PSWM (Table 3).

3.3.2. Shape of autotrophs

The aspect ratio showed the dominance of needle-shaped autotrophic microplankton (< 0.4) throughout the study (Figure 5; left side panel). The highest contribution of chain forms of *Skeletonema* sp., by abundance throughout the seasons, have a lower aspect ratio (<0.2). The relative dominance of *Chaetoceros* sp., *Leptocylindrus* sp., *Nitzschia* sp., *Fragilaria* sp., *Pleurosigma* sp., and *Pseudo-nitzschia* sp. contributed to the needle-shaped autotrophic microplankton. Similarly, *Odontella* sp., *Pediastrum* sp., and *Thalassiosira* sp., contributed to the spherical autotrophic microplankton (aspect ratio >0.6). Overall results suggested that needle-shaped autotrophs (aspect ratio < 0.4) predominated in the KBW throughout the year, whereas elliptical/spherical-shaped autotrophs dominated for a short period during SWM (aspect ratio >0.5; Figure 5a).

3.3.3. Heterotrophic micro-plankton

Throughout the study period, the heterotrophic micro-plankton community in the study area was dominated by the ciliate *Tintinnopsis* sp. The abundance and biomass were lowest during the SWM (av. 157 ± 81 L^{-1} and av. 1.33 ± 0.5 µgC L^{-1}), which increased during the NEM (av. 299 ± 88 L^{-1} and av. 3.19 ± 1.37 µgC L^{-1}) to peak during the PSWM (av. 725 ± 184 L^{-1} and 11.09 ± 3.39 µgC L^{-1}) (Figure 4). The PSWM peak was highly significant as compared to the other seasons (T-test, $p<0.05$). The mean size of individual micro-heterotrophs was lower during the SWM (av. 125185 ± 19802 µm³) and NEM (av. 152844 ± 23758 µm³), as compared to those during the PSWM (av. 201286 ± 11854 µm³), though there was no statistical significance (T-test, $p>0.2$; Table 2; Figure 4).

3.3.4. Shape of heterotrophs

Most of the organisms were elliptical/ spherical-shaped. Presence of *Gymnodinium* sp., *Protoperidinium* sp., *Strombidium* sp., *Favella* sp., copepod nauplius, and most of the rotifers contributed to the elliptical and spherical shape (aspect ratio >0.5; Figure 5; right side panel). Some species of *Tintinnopsis* having longer lorica and some elongated rotifers showed lower aspect ratio (0.2-0.4) indicating their spindle/ needle shape.

3.3.5. Micro-detritus and turbidity

Micro-detritus was quantified using the FlowCAM method, which showed the lowest quantity by volume during the SWM (av. 0.32 ± 0.08 mm^3 L^{-1}), increasing during the NEM (av. 0.54 ± 0.14 mm^3 L^{-1}) and PSWM (av. 0.47 ± 0.16 mm^3 L^{-1}) (Table 2). The abundance and distribution of detritus particles showed remarkable temporal and spatial variation (Figure 6a). The detritus abundance noticeably increased from SWM (av. 5890 ± 1933 L^{-1}) to the NEM (av. 11064 ± 4990 L^{-1}) and the PSWM (26389 ± 4979 L^{-1}) seasons (Table 2). The size of the detrital particles showed a noticeable

difference. The detritus volume was relatively high during January - April (Figure 6a). The SWM was characterized by very high turbidity (av. 22.1 ± 12.5 NTU) as compared to the NEM (av. 7.9 ± 5.3 NTU) and PSWM (av. 6.5 ± 5.1 NTU; Table 2).

3.3.6. Micro-detritus shape and size

The seasonality in particle diameter concerning the shape (Figure 6b-d) shows that most micro-detritus were <100 µm in diameter, and the spherical particles were more abundant than the needle-shaped ones. The emphatic dominance of spherical and elliptical-shaped particles over the needle-shaped particles throughout the year was observed in this study (Figure 6b-d). Though the dominant autotrophic microplankton was needle-shaped, the micro-detritus particles were spherical, indicting the effective aggregation of partially decomposed smaller organic particles and inorganic materials to form larger and elliptical detritus particles. The micrographs of detritus particles imaged in the FlowCAM (Figure 6e) appeared like the aggregation of semi-degraded particles.

3.4. Statistical results

As per the Shapiro-Wilk normality test, the homogenous datasets were tested with ANOVA and Tukey's HSD while the Kruskal-Wallis and Dunn's post hoc tests were applied to the heterogeneous datasets. The remarkable results of variance tests (Figure 7a-c) have been described in respective result sections. Figure 7d-e shows the multivariate correlation among the physicochemical and biological variables during different sampling periods. As evident from the tables and figures, the values of most biological parameters were higher during the PSWM, which is apparent from the RDA Triplot showing the projection of vectors pointing towards the PSWM sample points (Figure 7d). The relationship between nutrients and micro-autotrophs was found to be insignificant throughout the year, which is probably the result of excessive nutrients in the study region. The correlogram has been represented as pie charts along with correlation coefficients on both sides of a diagonal (Figure 7e). The coefficient values > 0.4 and < -0.4 indicate the significant relationship between the parameters ($p<0.05$).

4. Discussion

The southeastern Arabian Sea (SEAS) is found to sustain significantly higher phytoplankton biomass during SWM as compared to the rest of the period due to the coastal upwelling and river input (Jyothibabu et al., 2008; Asha Devi et al., 2010). The present study in the KBW contradicts this view with a distinctly high autotrophic micro-plankton abundance during PSWM. The primary reason for the marked contrast between the two systems has been explained below. The KBW is a eutrophic system, where nutrient concentrations are always in excess compared to what the natural

phytoplankton could assimilate; hence, nutrients are still excessively high in the water column. Therefore, even nutrient loading during SWM does not enhance the overall abundance and biomass of the phytoplankton community in KBW. On the other hand, the SEAS experiences a significant increase in the phytoplankton biomass due to the nutrient enrichment caused by coastal upwelling as compared to its nutrient-depleted PSWM levels (Subrahmanyam, 1959; Banse, 1982; Landry et al., 1998; Jyothibabu et al., 2008 and 2010; Karnan et al., 2017a). It was observed that the SEAS has the highest seasonal autotrophic biomass during the SWM, whereas the nutrient-depleted PSWM had very low phytoplankton biomass, significantly contributed by small-sized individuals (Karnan et al., 2020). Based on the above, the low standing stock of phytoplankton in the KBW during SWM can be attributed to three factors, (a) low solar radiation (PAR) in the water column (b) inefficiency of smaller plankton communities to utilize excess nutrients, and (c) phytoplankton cell acclimatization to the wide salinity fluctuations.

4.1. Photosynthetically Active Radiation (PAR)

It was observed in the past that the exposure of PAR in the KBW is significantly low during the SWM because of the high turbidity of the water column (Qasim et al., 1968; Jyothibabu et al., 2006; Madhu et al., 2007). The high river input also carries a large quantity of organic and inorganic forms of particulate matter to increase the turbidity of KBW. The suspended particulate matter (SPM) input into the Indian estuaries is highest during high rainfall and river runoff periods (Table 1; Qasim, 2003; Kumar and Sarma, 2018). During the present study, it was observed that light availability is restricted to a few centimetres to a meter in the water column during SWM due to high SPM and heavy cloud cover (at times) in the KBW (Qasim et al., 1968; Jyothibabu et al., 2006; Madhu et al., 2007). It was also observed that the high abundance and biomass of micro-autotrophs was during PSWM due to high solar radiation. Hence, the general understanding evolving from the present study is that PAR has a predominant role in controlling the abundance, biomass, and community composition of micro-autotrophs in the KBW.

4.2. Nutrient uptake by smaller micro-autotrophs

The SEAS sustains high phytoplankton biomass during the SWM due to the significant addition of nutrients through coastal upwelling (Banse, 1982; Menon et al., 2000; Jyothibabu et al., 2006; Asha Devi et al., 2010; Karnan et al., 2017a). In contrast, the phytoplankton in the KBW did not show a significant relation with macro-nutrients during the SWM (Sankaranarayanan and Qasim, 1969; Balachandran et al., 2005; Madhu et al., 2007). This indicated that fresh nutrients from the river influx were not efficiently assimilated by the smaller sized micro-autotrophs, which caused low

autotrophic micro-plankton biomass during the season. However, during the PSWM, more than threefold increase in autotrophic plankton biomass was observed, even though the nutrient level during the period was lower than the SWM. This observation delineates the crucial role played by PAR in enhancing the micro-autotrophic biomass, which was more robust than the effect of nutrients because nutrient concentration was always beyond the assimilation capacity of the native phytoplankton communities. However, the estuarine dynamics facilitated only the prevalence of dominant oligohaline smaller autotrophs in the KBW during the period.

4.3. Phytoplankton acclimatization to the salinity fluctuations

The KBW is dominated by fresh water during the SWM, with only its downstream region remaining brackish during the period. Hence, quite clearly, the estuarine phytoplankton community has to tolerate a wide range of salinity (Gopinathan, 1975; Brand, 1984; Menon et al., 2000). In the lower reaches of the backwater, as in the case of the present study, periodic salinity changes as a combined effect of fresh water influx and tidal action could be more pronounced compared to the rest of the regions of the backwater. The physiological responses of a low salinity phytoplankton community to high salinity intrusion could be the loss of water content and cell shrinkage through osmotic regulation (Kirst, 1990 and 1996). Similarly, osmotic acclimatization protects the marine phytoplankton from cell damage due to swelling and bursting while entering the low salinity regions of the backwater. The present study evidenced that the PSWM and early SWM were dominated by the mesohaline species of *Skeletonema*, *Thalassiosira*, *Eunotia*, *Staurastrum*, *Coelastrum,* and *Pediastrum*, which could acclimatize over a wide range of salinity. *Skeletonema* is euryhaline, and hence, can quickly acclimatize to medium salinity waters.

The abundance and biomass of micro-heterotrophs in the KBW was found to be the highest during the PSWM as compared to the rest of the period. The suitable environment such as salinity and food availability favour the survival and dominance of micro-heterotrophs in an aquatic ecosystem (Menon et al., 2000; Jyothibabu et al., 2006; 2008). They prefer to feed on pico- and nanoplankton, which are usually abundant in Indian waters during the PSWM period (Jyothibabu et al., 2006; 2013). The PSWM season seems to provide favourable conditions such as high salinity and abundance of pico- and nanoplankton communities, which supports the high stock of micro-heterotrophs, as noticed in the case of heterotrophic meso-plankton (Qasim, 1974; Madhupratap, 1987). The most abundant micro-heterotroph was the ciliate, *Tintinnopsis* sp., which is euryhaline and possesses a high level of tolerance to salinity (Jyothibabu et al., 2006). Also, it was observed in the present study that larger-sized micro-heterotrophs dominated the total biomass during the PSWM period, which can be comprehended with the following logic. Generally, in nutrient-rich waters,

larger-sized autotrophs dominate, supporting large-sized consumers such as fishes in the higher trophic levels (Karnan et al. 2017a). However, the backwater carries nutrient-rich water with low salinity and high turbidity, and this environmental setting cannot support the efficient production of larger autotrophs. Alternately, it leads to the dominance of smaller autotrophs, which can be efficiently fed upon by micro-heterotrophs such as microzooplankton. The dominance of smaller-sized plankton communities shows that the estuarine food web transfers a large portion of energy through microbial food web pathways during most of the year, and the role of the traditional food chain is relatively smaller in the KBW (Figure 8; Jyothibabu et al., 2006).

During the SWM, the floodwater brings a large quantity of suspended particulate matter into the KBW, which causes high turbidity in the water column. Qasim and Sankaranarayanan (1972) quantified the detritus matter in the lower reaches of KBW using sediment traps deployed at ~0.5m above the bottom. These sediment traps collected the total particles settled in the water column and, therefore, the total suspended matter was found to be higher during the SWM. On the other hand, the total organic detritus was higher during the PSWM condition. In 1970s, it seemed to be a contradiction; however, in the present study, it is evident that the abundance of the micro-detritus in the water column is lower during the SWM compared to the rest of the periods. Several studies reported that the significant contribution of suspended material to the estuaries during the monsoon seasons is allochthonous and during non-monsoon seasons, it is autochthonous (Onstad et al., 2000; Sanchez-Vidal et al., 2013; Kumar and Sarma, 2018). A part of the organic detritus in the suspended materials get decomposed by the heterotrophic bacteria or consumed by the detritivorous organisms, while the remaining either settle down to the bottom or are exported to the adjacent coastal regions (Joseph and Kurup, 1989; Jyothibabu et al., 2006). The high availability of organic detritus in estuaries also leads to an increase in heterotrophic bacterial biomass, which in turn, strengthens the microbial food chain (Figure 8; Fenchel and Jorgensen, 1977; Jyothibabu et al., 2006; Mayor et al., 2014). Heterotrophic bacteria are the initiators of the microbial food chains, which are more abundant in the organic detritus as compared to the water mass (Turner, 2002; Jyothibabu et al., 2006). The detritus are also consumed by ciliates and heterotrophic flagellates and thus it functions as a significant part in the microbial food web (Mayor et al., 2014). The dominance of smaller-sized autotrophic plankton throughout the year, along with abundant organic detritus in the KBW, indicates a dominant microbial food web in the system (Figure 8; Azam et al., 1983; Jyothibabu et al., 2006; Mohan et al., 2016).

The present study also signifies the fact that the low PAR in the KBW during the SWM is mainly caused by the high amount of clays and mineral particles rather than the organic micro-detritus. The

coloured dissolved organic matter (CDOM) released during mass death of macrophytes and degradation of biological matters can also cause attenuation of light in estuaries (Stabenau et al., 2004; Branco and Kremer, 2005; Yamashita and Tanoue, 2008; Nelson and Siegel, 2013). The major macrophyte found in the KBW is *Eichhornia*, which blooms during the SWM and vanishes under high salinity conditions. However, it did not influence the turbidity since the present study showed a significant correlation between organic micro-detritus and microplankton (both auto- and heterotrophs). Jyothibabu et al., (2006) showed that the plankton food web in the KBW is most active during the non-monsoon periods due to an increase in the abundance of large-sized consumers (herbivores, omnivores, and carnivores). The role of organic detritus in sustaining the detritivores in pelagic, as well as benthic ecosystems, is well established (Fenchel and Jorgensen, 1977; Gowing and Wishner, 1992; Moore et al., 2004; Attayde and Ripa, 2008; Mayor et al., 2014; Anderson et al., 2017). Based on the present study, it is proposed that in addition to a dominant plankton food web, a detritus-sourced food chain is also more dominant in the KBW during the non-monsoon periods (Figure 8). This could be the main reason for the high living resource potential of KBW during the non-monsoon period compared to the monsoon (Qasim et al., 1974; Menon et al., 2000; Madhu et al., 2010; Sooria et al., 2015).

5. Conclusion

This study quantifies the micro-plankton (both autotrophic and heterotrophic) and micro-detritus, and it explains their role in structuring the food web dynamics of a tropical monsoonal estuary such as KBW. During this year-long study, samples were collected fortnightly from the KBW and analyzed using FlowCAM. The smaller-sized micro-plankton community was found dominant and persistent in the study area throughout the year. The micro-plankton community, especially *Skeletonema* sp., was found to be dominant and persistent throughout the year. The size and growth of micro-autotrophs were severely limited by hydrographical parameters such as PAR and salinity, whereas nutrients showed no impact. The abundance and biomass of micro-autotrophs were very high during PSWM when PAR was very high. Therefore, an increase in the micro-detritus could well be due to a corresponding increase in the microplankton in KBW. The concomitant abundances of micro-plankton and micro-detritus during PSWM and NEM periods are indicative of an active microbial food web, which increased the biological productivity of the estuary, in general.

Acknowledgements

The authors thank the Director of CSIR - National Institute of Oceanography, India, for facilities and encouragement. The first author thanks CSIR, India, for providing research fellowship during the

period of this work. This work was conducted under the project of 'Ocean Finder' carried out by CSIR-NIO. This is CSIR-NIO contribution number.....

References

Acharyya, T., Sarma, V., Sridevi, B., Venkataramana, V., Bharathi, M.D., Naidu, S.A., Kumar, B.S.K., Prasad, V.R., Bandyopadhyay, D., Reddy, N.P.C., 2012. Reduced river discharge intensifies phytoplankton bloom in Godavari estuary, India. Mar. Chem. 132, 15-22.

Alvarez, E., Lopez-Urrutia, A., Nogueira, E., 2012. Improvement of plankton biovolume estimates derived from image-based automatic sampling devices: application to FlowCAM. J. Plankton Res. 34, 454-469.

Alvarez, E., Lopez-Urrutia, A., Nogueira, E., Fraga, S., 2011. How to effectively sample the plankton size spectrum? A case study using FlowCAM. J. Plankton Res. 33, 1119-1133.

Anderson, T.R., Pond, D.W., Mayor, D.J., 2017. The role of microbes in the nutrition of detritivorous invertebrates: a stoichiometric analysis. Front. Microbiol. 7, 2113.

Anilkumar, N., Revichandran, C., Sankaranarayanan, V.N., Josanto, V., 1998. Residual fluxes of water, salt and suspended sediment in the Beypore estuary. Indian J. Mar. Sci. 27, 157-162.

Asha Devi, C.R., Jyothibabu, R., Sabu, P., Jacob, J., Habeebrehman, H., Prabhakaran, M.P., Jayalakshmi, K.J., Achuthankutty, C.T., 2010. Seasonal variations and trophic ecology of microzooplankton in the southeastern Arabian Sea. Cont. Shelf Res. 30, 1070-1084.

Attayde, J.L., Ripa, J., 2008. The coupling between grazing and detritus food chains and the strength of trophic cascades across a gradient of nutrient enrichment. Ecosystems 11, 980-990.

Azam, F., Fenche, T., Field, J.G., Gra, J.S., Meyer-Rei, L.A., Thingstad, F., 1983. The ecological role of water-column microbes in the sea. Mar. Ecol. Prog. Ser. 10, 257-263.

Balachandran, K.K., Joseph, T., Nair, M., Sankaranarayanan, V.N., Kesavadas, V., Sheeba, P., 2003. Geochemistry of surficial sediments along the central southwest coast of India: Seasonal changes in regional distribution. J. Coastal Res. 19, 664-683.

Balachandran, K.K., Raj, C.M.L., Nair, M., Joseph, T., Sheeba, P., Venugopal, P., 2005. Heavy metal accumulation in a flow restricted, tropical estuary. Estuar. Coast. Shelf Sci. 65, 361-370.

Banse, K., 1982. Mass-scaled rates of respiration and intrinsic growth in very small invertebrates. Mar. Ecol. Prog. Ser. 9, 281-297.

Branco, A.B., Kremer, J.N., 2005. The relative importance of chlorophyll and colored dissolved organic matter (CDOM) to the prediction of the diffuse attenuation coefficient in shallow estuaries. Estuaries 28, 643-652.

Brand, L.E., 1984. The salinity tolerance of forty-six marine phytoplankton isolates. Estuar. Coast. Shelf Sci. 18, 543-556.

Caromel, A.G.M., Schmidt, D.N., Phillips, J.C., Rayfield, E.J., 2014. Hydrodynamic constraints on the evolution and ecology of planktic foraminifera. Mar. Micropaleontol. 106, 69-78.

Crawford, C.B., Quinn, B., 2017. Microplastic identification techniques, in: Crawford, C.B., Quinn, B. (Eds.), Microplastic Pollutants. Elsevier.

Davis, C.S., Hu, Q., Gallager, S.M., Tang, X., Ashjian, C.J., 2004. Real-time observation of taxa-specific plankton distributions: an optical sampling method. Mar. Ecol. Prog. Ser. 284, 77-96.

Fenchel, T.M., Jorrgensen, B.B., 1977. Detritus food chains of aquatic ecosystems: The Role of Bacteria, in: Alexander, M. (Ed.), Adv Microb Ecol. Springer, Boston, MA, pp. 1-58.

FlowCAM Manual, 2009. Fluid Imaging Technologies. Yarmouth, Maine, pp. 1-121.

Friendly, M., 2002. Corrgrams: Exploratory displays for correlation matrices. The American Statistician 56, 316-324.

Gopinathan, C.P., 1975. Studies on the estuarine diatoms of India. Bulletin of the Department of Marine Sciences, University of Cochin 7, 995-1004.

Gowing, M.M., Garrison, D.L., Wishner, K.F., Gelfman, C., 2003. Mesopelagic microplankton of the Arabian Sea. Deep Sea Res. Part I Oceanogr. Res. Pap. 50, 1205-1234.

Gowing, M.M., Wishner, K.F., 1992. Feeding ecology of benthopelagic zooplankton on an eastern tropical Pacific seamount. Mar. Biol. 112, 451-467.

Grasshoff, K., Ehrhardt, M., Kremling, K., 1983. Methods of Seawater Analysis (Eds.). Verlag Chemie, Weinheim, 89–224.

Jose, J., Giridhar, R., Anas, A., Bharathi, P.A.L., Nair, S., 2011. Heavy metal pollution exerts reduction/adaptation in the diversity and enzyme expression profile of heterotrophic bacteria in Cochin estuary, India. Environ. Pollut. 159, 2775-2780.

Joseph, J., Kurup, P.G., 1989. Volume transport and estuarine features at Cochin inlet. Mahasagar 22, 165-172.

Jyothibabu, R., Devi, C.R.A., Madhu, N.V., Sabu, P., Jayalakshmy, K.V., Jacob, J., Habeebrehman, H., Prabhakaran, M.P., Balasubramanian, T., Nair, K.K.C., 2008. The response of microzooplankton (20-200μm) to coastal upwelling and summer stratification in the southeastern Arabian Sea. Cont. Shelf Res. 28, 653-671.

Jyothibabu, R., Madhu, N.V., Habeebrehman, H., Jayalakshmy, K.V., Nair, K.K.C., Achuthankutty, C.T., 2010. Re-evaluation of 'paradox of mesozooplankton' in the eastern Arabian Sea based on ship and satellite observations. J. Mar. Syst. 81, 235-251.

Jyothibabu, R., Madhu, N.V., Jayalakshmi, K.V., Balachandran, K.K., Shiyas, C.A., Martin, G.D., Nair, K.K.C., 2006. Impact of freshwater influx on microzooplankton mediated food web in a tropical estuary (Cochin backwaters-India). Estuar. Coast. Shelf Sci. 69, 505-518.

Jyothibabu, R., Mohan, A.P., Jagadeesan, L., Anjusha, A., Muraleedharan, K.R., Lallu, K.R., Kiran, K., Ullas, N., 2013. Ecology and trophic preference of picoplankton and nanoplankton in the Gulf of Mannar and the Palk Bay, southeast coast of India. J. Mar. Syst. 111, 29-44.

Karnan, C., Jyothibabu, R., Arunpandi, N., Albin, K.J., Parthasarathi, S., Krishnan, S.S., 2020. Response of microplankton size structure to summer stratification, freshwater influx and coastal upwelling in the Southeastern Arabian Sea. Cont. Shelf Res. 193, 104038.

Karnan, C., Jyothibabu, R., Arunpandi, N., Jagadeesan, L., Muraleedharan, K.R., Pratihari, A.K., Balachandran, K.K., Naqvi, S.W.A., 2017a. Discriminating the biophysical impacts of coastal upwelling and mud banks along the southwest coast of India. J. Mar. Syst. 172, 24-42.

Karnan, C., Jyothibabu, R., Manoj Kumar, T.M., Arunpandi, N., Jagadeesan, L., 2017b. On the Accuracy of Assessing Copepod Size and Biovolume using FlowCAM and Traditional Microscopy. Indian J. Mar. Sci. 46, 1261-1264.

Karp-Boss, L., Boss, E., 2016. The elongated, the squat and the spherical: selective pressures for phytoplankton shape, Aquatic microbial ecology and biogeochemistry: a dual perspective. Springer, pp. 25-34.

Kirst, G., 1990. Salinity tolerance of eukaryotic marine algae. Annu. Rev. Plant Biol. 41, 21-53.

Kirst, G., 1996. Osmotic adjustment in phytoplankton and macroalgae, Biological and environmental chemistry of DMSP and related sulfonium compounds. Springer, pp. 121-129.

Kumar, B.S.K., Sarma, V., 2018. Variations in concentrations and sources of bioavailable organic compounds in the Indian estuaries and their fluxes to coastal waters. Cont. Shelf Res. 166, 22-33.

Kumar, L.A., Thangaradjou, T., Kannan, L., 2006. Physico-chemical and biological properties of the Muthupettai Mangrove in, Tamil Nadu. J. Mar. Biol. Assoc. India, 131-138.

Kumari, V.R., Rao, I.M., 2010. Suspended sediment dynamics in Krishna estuary, east coast of India. Indian J. Mar. Sci. 39, 248-256.

Landry, M.R., Brown, S.L., Campbell, L., Constantinou, J., Liu, H., 1998. Spatial patterns in phytoplankton growth and microzooplankton grazing in the Arabian Sea during monsoon forcing. Deep Sea Res. Part II Top. Stud. Oceanogr. 45, 2353-2368.

Leps, J., Smilauer, P., 2003. Multivariate analysis of ecological data using CANOCO. Cambridge University Press.

Loder, M.G.J., Gerdts, G., 2015. Methodology used for the detection and identification of microplastics-A critical appraisal, in: Bergmann, M. (Ed.), Marine anthropogenic litter. Springer, pp. 201-227.

Madhu, N.V., Jyothibabu, R., Balachandran, K.K., 2010. Monsoon-induced changes in the size-fractionated phytoplankton biomass and production rate in the estuarine and coastal waters of southwest coast of India. Environ. Monit. Assess. 166, 521-528.

Madhu, N.V., Jyothibabu, R., Balachandran, K.K., Honey, U.K., Martin, G.D., Vijay, J.G., Shiyas, C.A., Gupta, G.V.M., Achuthankutty, C.T., 2007. Monsoonal impact on planktonic standing stock and abundance in a tropical estuary (Cochin backwaters-India). Estuar. Coast. Shelf Sci. 73, 54-64.

Madhupratap, M., 1987. Status and strategy of zooplankton of tropical Indian estuaries: A review. Bull. Plankton Soc. Jpn. 34, 65-81.

Marquis, E., Niquil, N., Dupuy, C., 2011. Does the study of microzooplankton community size structure effectively define their dynamics? Investigation in the Bay of Biscay (France). J. Plankton Res. 33, 1104-1118.

Martin, G., Muraleedharan, K., Vijay, J., Rejomon, G., Madhu, N., Shivaprasad, A., Haridevi, C., Nair, M., Balachandran, K., Revichandran, C., 2010. Formation of anoxia and denitrification in the bottom waters of a tropical estuary, southwest coast of India. Biogeosci. Disc. 7, 1751-1782.

Mayor, D.J., Sanders, R., Giering, S.L.C., Anderson, T.R., 2014. Microbial gardening in the ocean's twilight zone: Detritivorous metazoans benefit from fragmenting, rather than ingesting, sinking detritus: Fragmentation of refractory detritus by zooplankton beneath the euphotic zone stimulates the harvestable production of labile and nutritious microbial biomass. Bioessays 36, 1132-1137.

Menden-Deuer, S., Lessard, E.J., 2000. Carbon to volume relationships for dinoflagellates, diatoms, and other protist plankton. Limnol. Oceanogr. 45, 569-579.

Menon, N.N., Balchand, A.N., Menon, N.R., 2000. Hydrobiology of the Cochin backwater system-a review. Hydrobiologia 430, 149-183.

Michaels, A.F., Caron, D.A., Swanberg, N.R., Howse, F.A., Michaels, C.M., 1995. Planktonic sarcodines (Acantharia, Radiolaria, Foraminifera) in surface waters near Bermuda: abundance, biomass and vertical flux. J. Plankton Res. 17, 131-163.

Mohan, A.P., Jyothibabu, R., Jagadeesan, L., Lallu, K., Karnan, C., 2016. Summer monsoon onset-induced changes of autotrophic pico-and nanoplankton in the largest monsoonal estuary along the west coast of India. Environ. Monit. Assess. 188, 93.

Moore, J.C., Berlow, E.L., Coleman, D.C., de Ruiter, P.C., Dong, Q., Hastings, A., Johnson, N.C., McCann, K.S., Melville, K., Morin, P.J., 2004. Detritus, trophic dynamics and biodiversity. Ecol. Lett. 7, 584-600.

Mukhopadhyay, S.K., Biswas, H., De, T.K., Jana, T.K., 2006. Fluxes of nutrients from the tropical River Hooghly at the land-ocean boundary of Sundarbans, NE Coast of Bay of Bengal, India. J. Mar. Syst. 62, 9-21.

Nelson, N.B., Siegel, D.A., 2013. The global distribution and dynamics of chromophoric dissolved organic matter. Annu. Rev. Mar. Sci. 5, 447-476.

Olson, E., 2011a. Particle shape factors and their use in image analysis part 1: theory. J. GXP Compl. 15, 85.

Olson, E., 2011b. Particle shape factors and their use in image analysis part II: practical applications. J. GXP Compl. 15, 77.

Onstad, G.D., Canfield, D.E., Quay, P.D., Hedges, J.I., 2000. Sources of particulate organic matter in rivers from the continental USA: lignin phenol and stable carbon isotope compositions. Geochim. Cosmochim. Acta 64, 3539-3546.

Parvathi, A., Jasna, V., Haridevi, K.C., Jina, S., Greeshma, M., Breezy, J., Nair, M., 2013. Diurnal variations in bacterial and viral production in Cochin estuary, India. Environ. Monit. Assess. 185, 8077-8088.

Qasim, S.Z., 2003. Indian estuaries. Allied publishers, New Delhi.

Qasim, S.Z., Bhattathiri, P.M.A., Abidi, S.A.H., 1968. Solar radiation and its penetration in a tropical estuary. J. Exp. Mar. Biol. Ecol. 2, 87-103.

Qasim, S.Z., Bhattathiri, P.M.A., Devassy, V.P., 1972. The influence of salinity on the rate of photosynthesis and abundance of some tropical phytoplankton. Mar. Biol. 12, 200-206.

Qasim, S.Z., Sankaranarayanan, V.N., 1972. Organic detritus of a tropical estuary. Mar. Biol. 15, 193-199.

Qasim, S.Z., Vijayaraghavan, S., Joseph, K.J., Balachandran, V.K., 1974. Contribution of microplankton and nannoplankton in the waters of a tropical estuary. Indian J. Mar. Sci. 3, 146-149.

R Core Team, 2013. R: A language and environment for statistical computing.

Ramamirtham, C., Jayaraman, R., 1963. Some aspects of the hydrographical conditions of the backwaters around Willingdon Island (Cochin). J. Mar. Biol. Assoc. India 5, 170-177.

Rao, V.P., Shynu, R., Kessarkar, P.M., Sundar, D., Michael, G.S., Narvekar, T., Blossom, V., Mehra, P., 2011. Suspended sediment dynamics on a seasonal scale in the Mandovi and Zuari estuaries, central west coast of India. Estuar. Coast. Shelf Sci. 91, 78-86.

Ray, S.B., Mohanti, M., Somayajulu, B.L.K., 1984. Suspended matter, major cations and dissolved silicon in the estuarine waters of the Mahanadi river, India. J. Hydrol. 69, 183-196.

Sanchez-Vidal, A., Higueras, M., Marti, E., Liquete, C., Calafat, A., Kerherve, P., Canals, M., 2013. Riverine transport of terrestrial organic matter to the North Catalan margin, NW Mediterranean Sea. Prog. Oceanogr. 118, 71-80.

Sankaranarayanan, V.N., Qasim, S.Z., 1969. Nutrients of the Cochin backwater in relation to environmental characteristics. Mar. Biol. 2, 236-247.

Sarma, V., Gupta, S.N.M., Babu, P.V.R., Acharya, T., Harikrishnachari, N., Vishnuvardhan, K., Rao, N.S., Reddy, N.P.C., Sarma, V.V., Sadhuram, Y., 2009. Influence of river discharge on plankton metabolic rates in the tropical monsoon driven Godavari estuary, India. Estuar. Coast. Shelf Sci. 85, 515-524.

Sooria, P.M., Jyothibabu, R., Anjusha, A., Vineetha, G., Vinita, J., Lallu, K.R., Paul, M., Jagadeesan, L., 2015. Plankton food web and its seasonal dynamics in a large monsoonal estuary (Cochin backwaters, India)-significance of mesohaline region. Environ. Monit. Assess. 187, 1-22.

Sosik, H.M., Olson, R.J., 2007. Automated taxonomic classification of phytoplankton sampled with imaging-in-flow cytometry. Limnol. Oceanogr. Methods 5, 204-216.

Stabenau, E.R., Zepp, R.G., Bartels, E., Zika, R.G., 2004. Role of the seagrass Thalassia testudinum as a source of chromophoric dissolvedorganic matter in coastal south Florida. Mar. Ecol. Prog. Ser. 282, 59-72.

Subrahmanyam, R., 1959. Studies on the phytoplankton of the west coast of india. Proc. Indian Acad. Sci. Sec. B Part I, 508, 189-252.

Tada, K., Pithakpol, S., Yano, R., Montani, S., 2000. Carbon and nitrogen content of Noctiluca scintillans in the Seto Inland Sea, Japan. J. Plankton Res. 22, 1203-1211.

Tomas, C., Hasle, G., Syvertsen, E., Steidinger, K., Tangen, K., 1996. Identifying Marine Diatoms and Dinoflagellates. Academic Press, San Diego.

Turner, J.T., 2002. Zooplankton fecal pellets, marine snow and sinking phytoplankton blooms. Aquat. Microb. Ecol. 27, 57-102.

Verity, P.G., Lagdon, C., 1984. Relationships between lorica volume, carbon, nitrogen, and ATP content of tintinnids in Narragansett Bay. J. Plankton Res. 6, 859-868.

Verity, P.G., Robertson, C.Y., Tronzo, C.R., Andrews, M.G., Nelson, J.R., Sieracki, M.E., 1992. Relationships between cell volume and the carbon and nitrogen content of marine photosynthetic nanoplankton. Limnol. Oceanogr. 37, 1434-1446.

Yamashita, Y., Tanoue, E., 2008. Production of bio-refractory fluorescent dissolved organic matter in the ocean interior. Nat. Geosci. 1, 579.

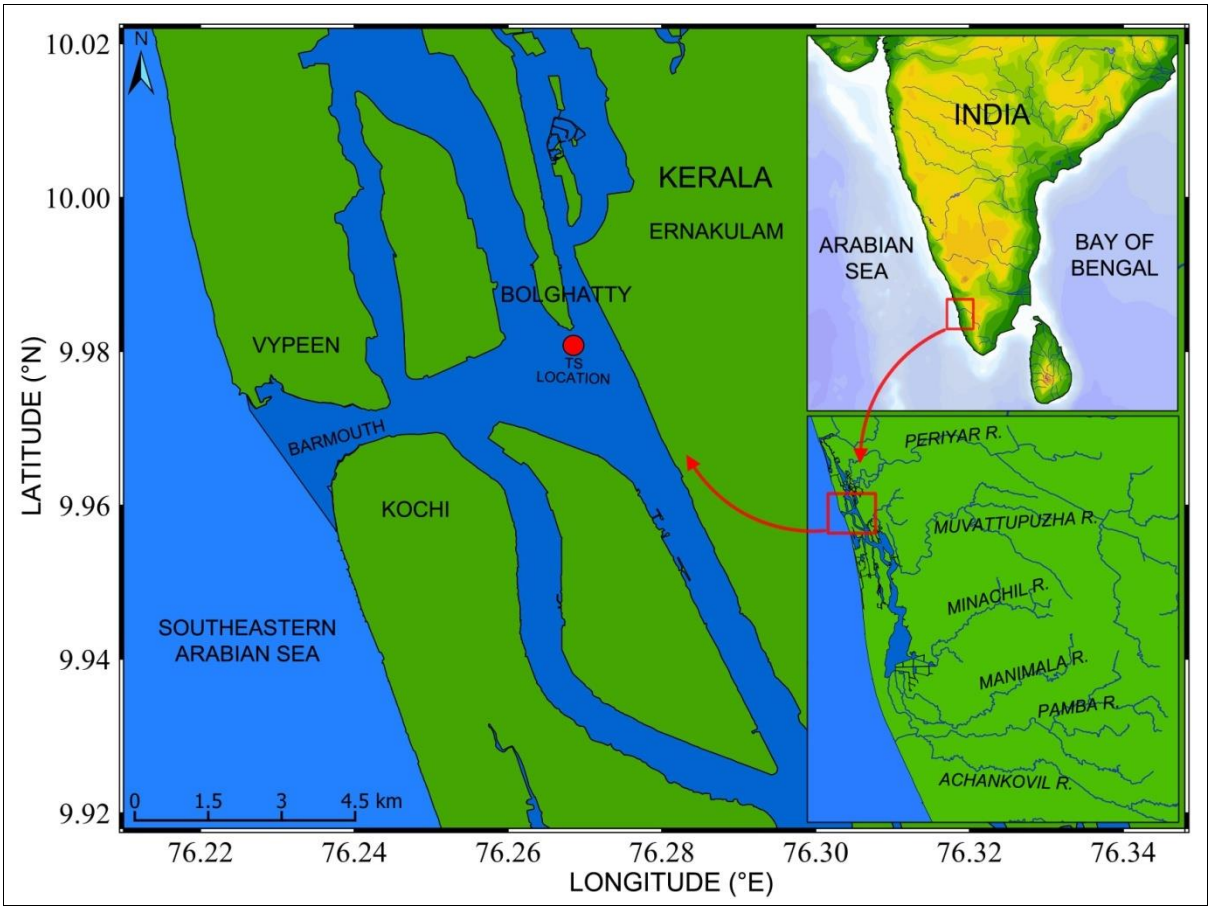

Figure 1- Time series sampling location (red bullet) in the downstream of Kochi backwaters. The lower inset map representing major rivers.

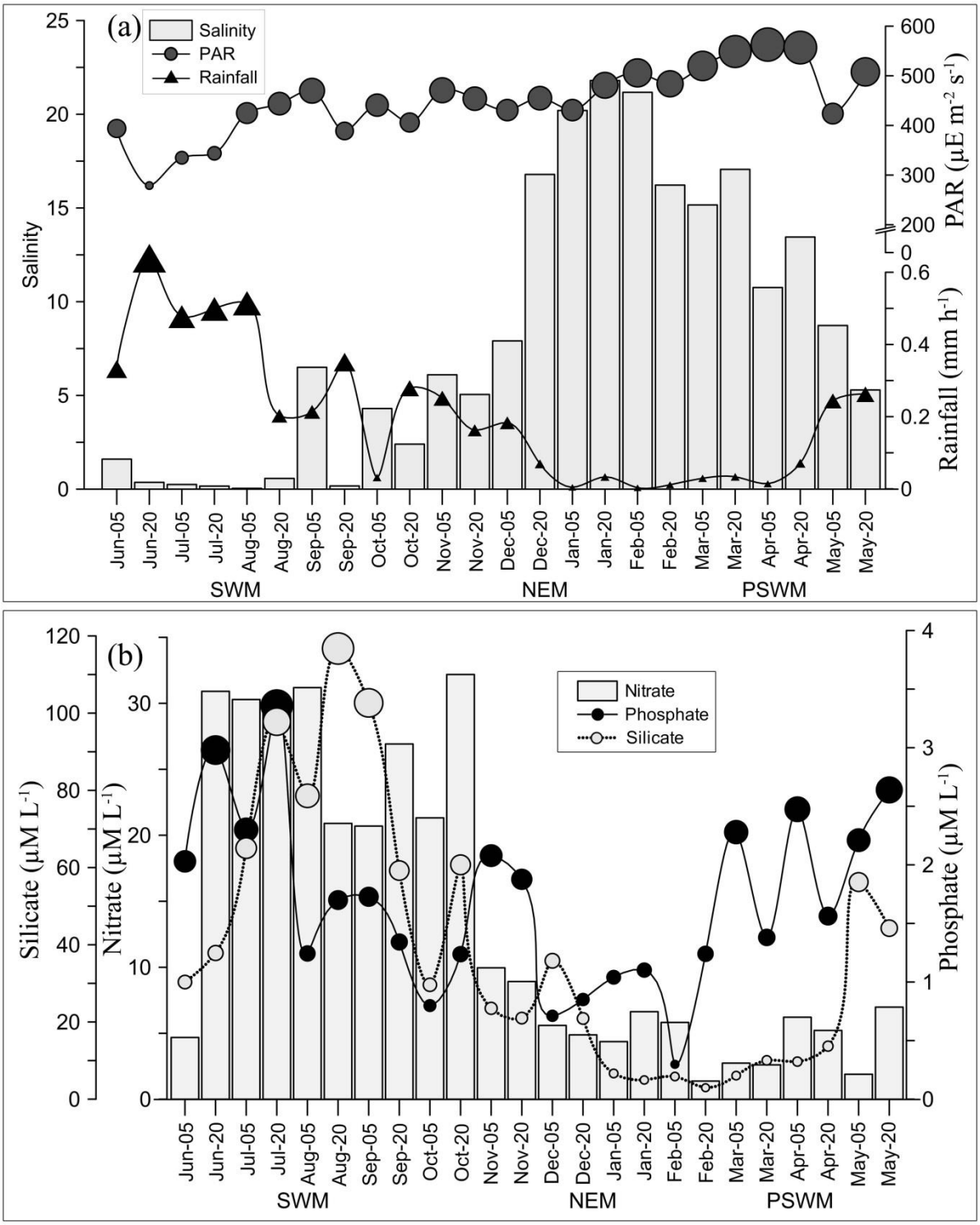

Figure 2 – Annual hydrography of Kochi backwaters, (a) physical parameters (PAR, rainfall and salinity), and (b) concentration of macro-nutrients (nitrate, phosphate and silicate).

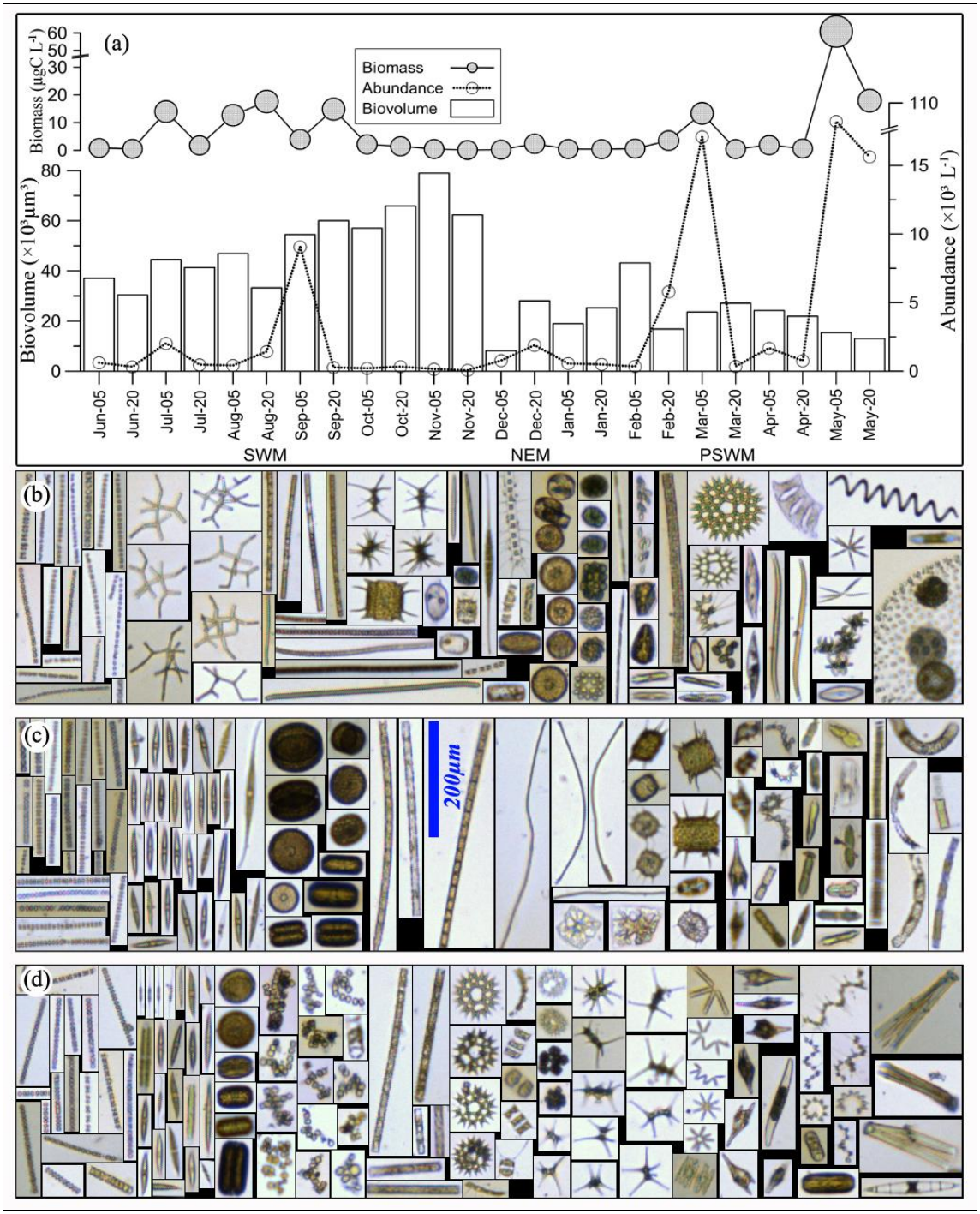

Figure 3 – (a) Autotrophic microplankton abundance, biomass and biovolume, and FlowCAM images of micro-autotrophs found higher during (b) SWM, (c) NEM and (d) PSWM.

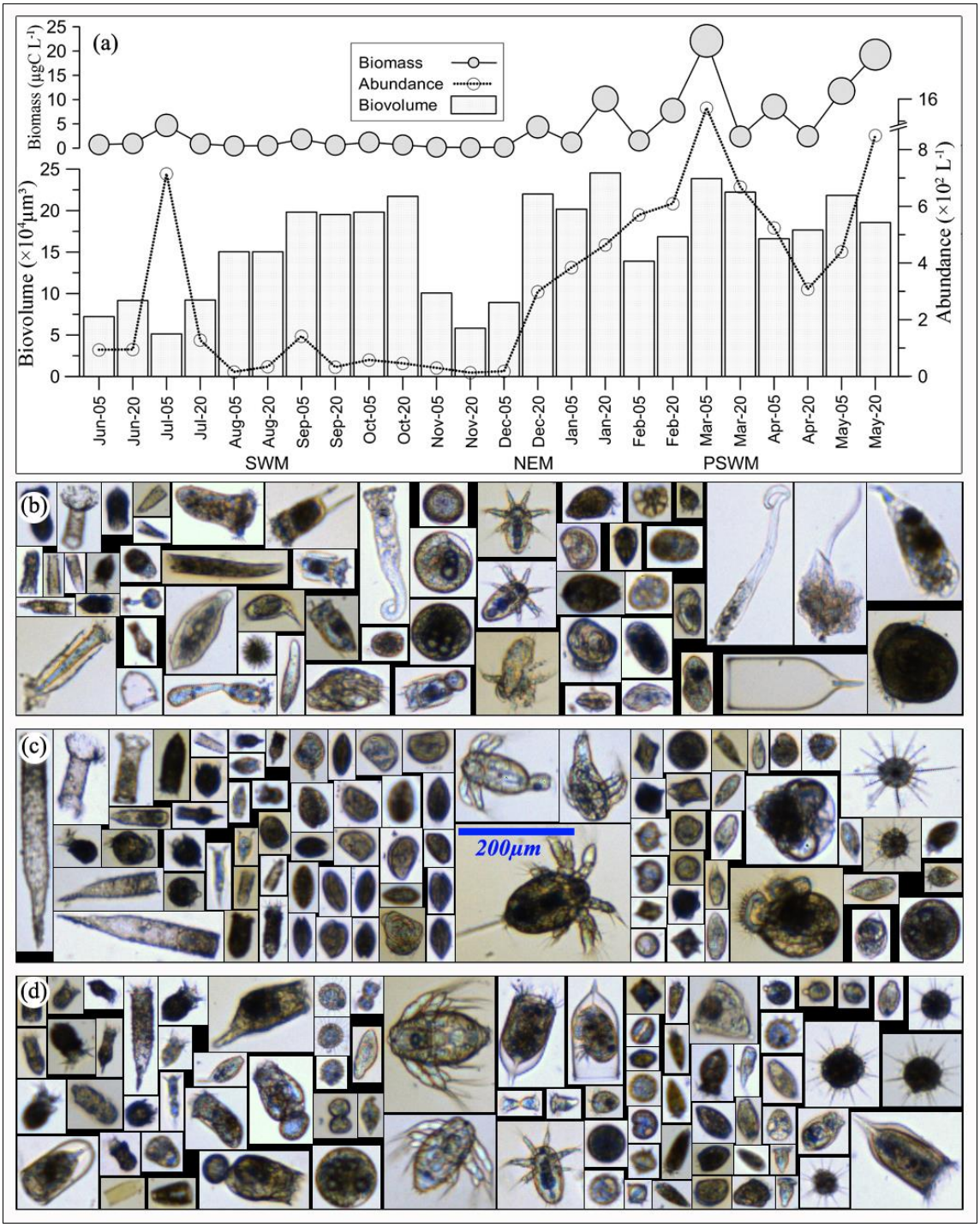

Figure 4 – (a) Heterotrophic micro-plankton abundance, biomass and biovolume and, FlowCAM images of micro-heterotrophs found higher during (b) SWM, (c) NEM and (d) PSWM.

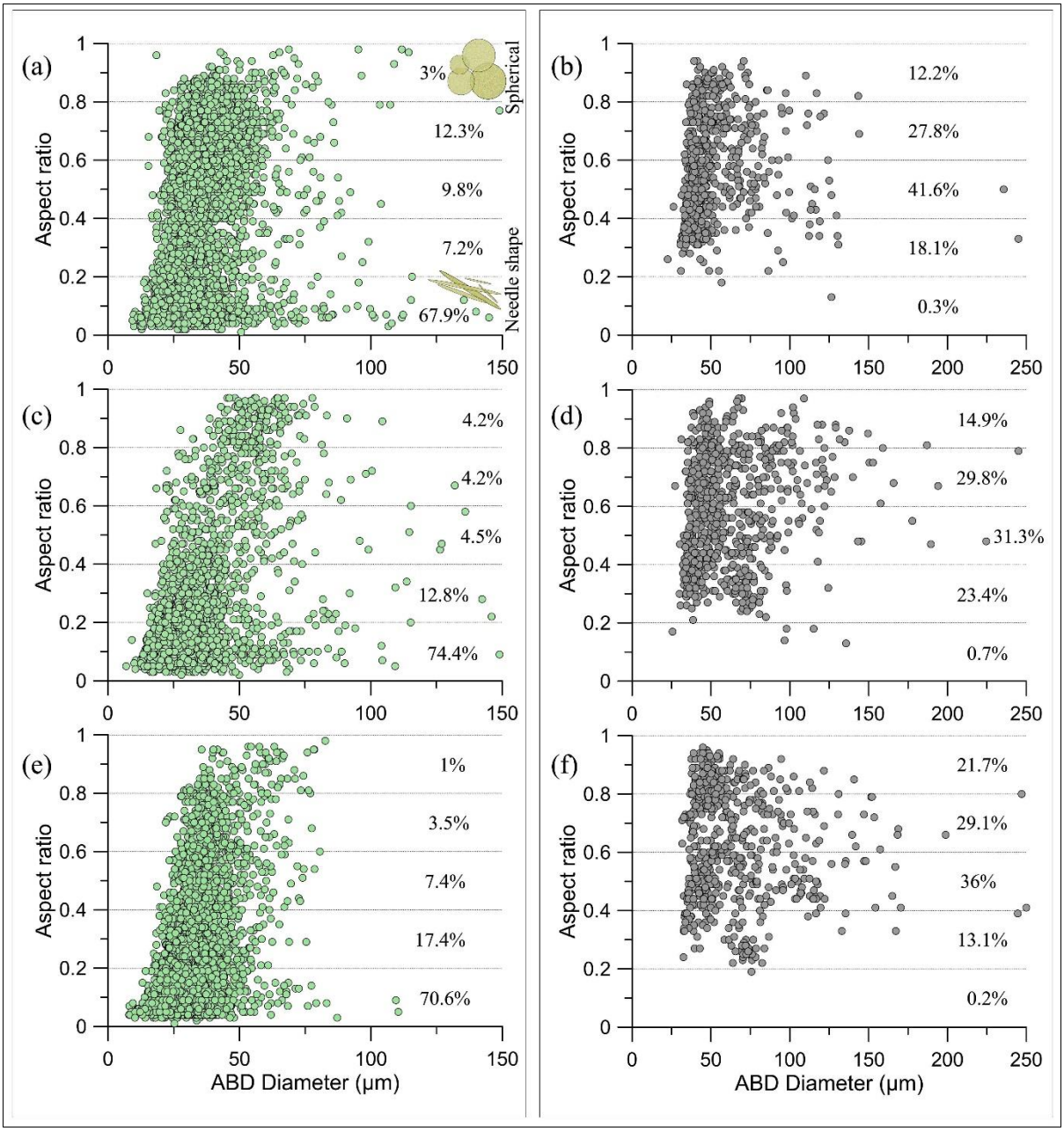

Figure 5 – The microplankton size (diameter) with respect to their shape (aspect ratio) presented for autotrophs (left side panels) and heterotrophs (right side panels) during (a-b) SWM, (c-d) NEM and (e-f) PSWM. In panel (a), model shapes given to showspherical shape (aspect ratio>0.6) and needle shape (aspect ratio<0.4), and the respective quantity of plankton contribution given in percentage.It shows the dominance of needle shaped autotrophic micro-plankton in the KBW throughout the year and a noticeable increase of spherical shaped plankton found during SWM (panel a).The heterotrophic micro-plankton showed higher percentage in elliptical to spherical shaped and needles shaped animals were negligible.

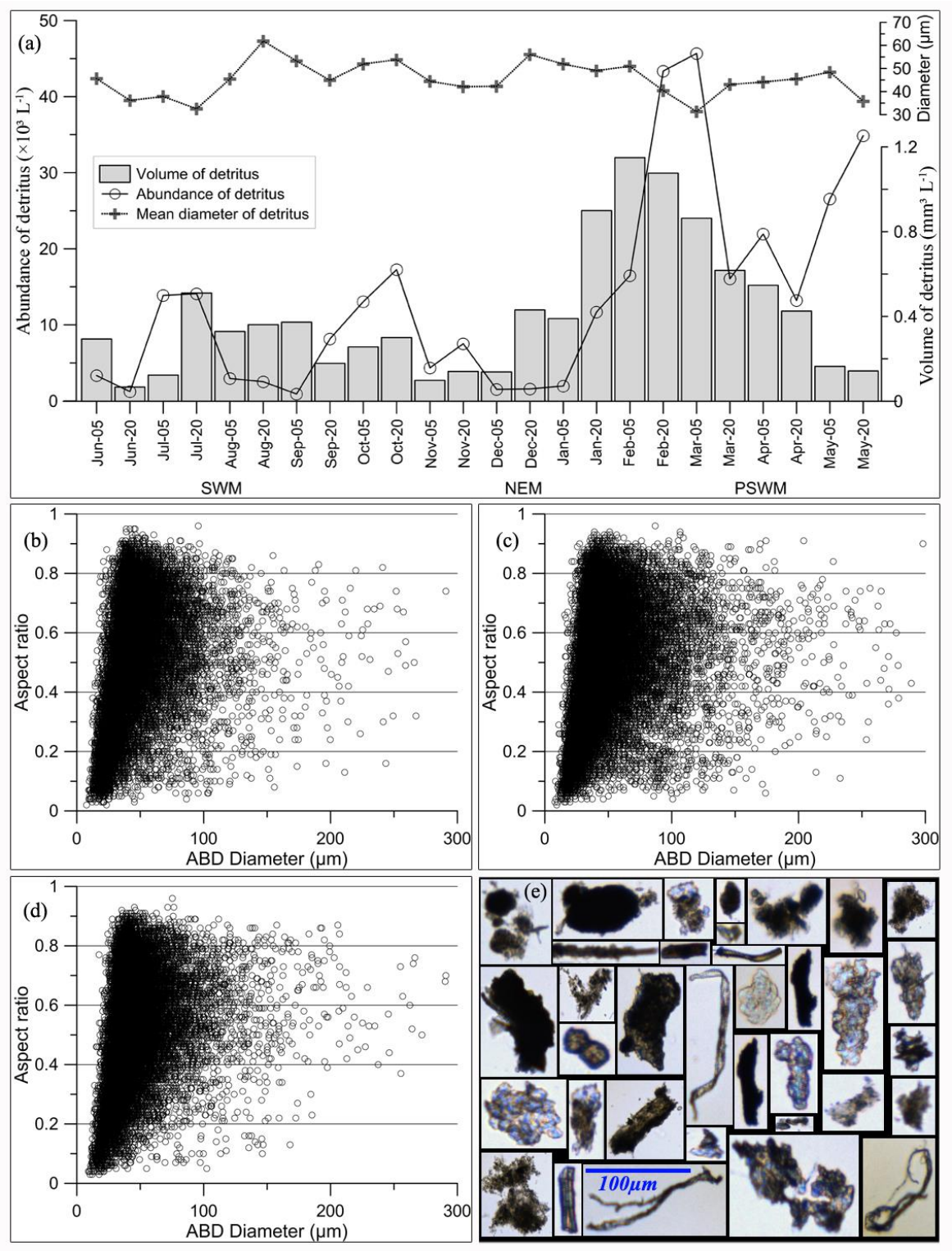

Figure 6 - (a) The abundance, volume and mean size of detritus during the fortnight sampling session and, detritus size (ABD diameter) distribution with respect to their aspect ratio during (b) SWM, (c) NEM and (d) PSWM. The aspect ratio of detritus towards 0 indicates acicular/needle shaped particles and towards 1 indicates spherical/round shaped particles.

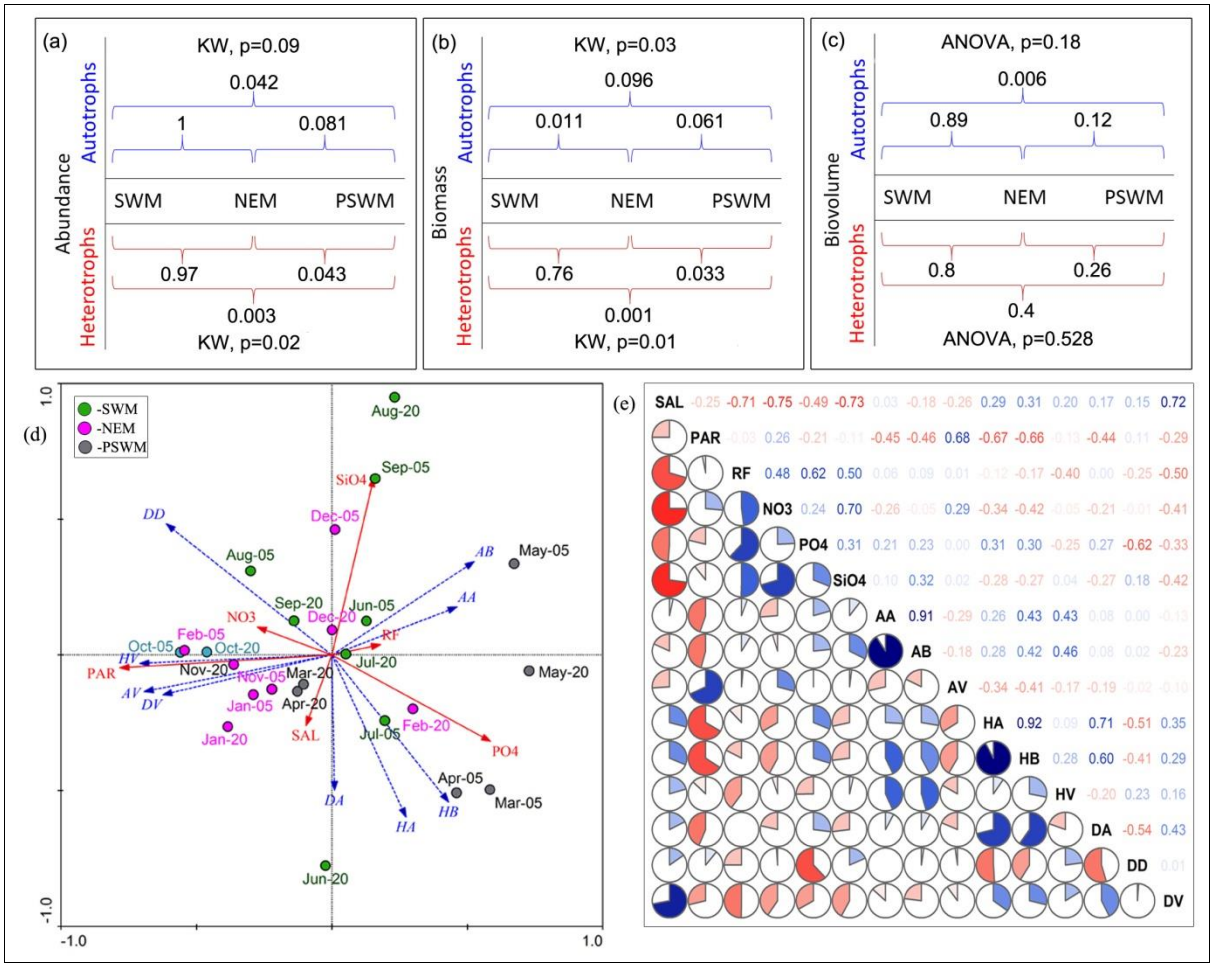

Figure 7 – The inter- and multi-seasonal comparison of plankton variables with level of variance (p-value; upper panels), (a) abundance of autotrophs (blue font) and heterotrophs (red font), (b) biomass and (c) biovolume, respectively. The significance of variation is represented by stating the p-values (refer methods section for type of analysis). The analysis done in RStudio (ggboxplot package) and the figure was redrawn to avoid data replication. The lower panels representing multivariate correlation analysis (d) RDA Triplot shows the inter-relationships among various parameters during different sampling periods and (e) the correlation matrix represented as pie charts in the lower left diagonal and respective correlation coefficients on the upper right diagonal (plotted in R-Studio; corrgram). The colour codes, red indicates negative, blue indicates positive and pale colour indicates weak correlation. The coefficient values > 0.4 and < -0.4 indicate significant correlation ($p<0.05$). Abbreviations, SAL: salinity, PAR: photosynthetically available radiation, RF: rainfall, NO3: nitrate, PO4: phosphate, SiO4: silicate, AA: abundance of autotrophs, AB: biomass of autotrophs, AV: biovolume of autotrophs, HA: abundance of heterotrophs, HB: biomass of heterotrophs, HV: biovolume of heterotrophs, DA: abundance of detritus, DD: diameter of detritus and DV: volume of detritus.

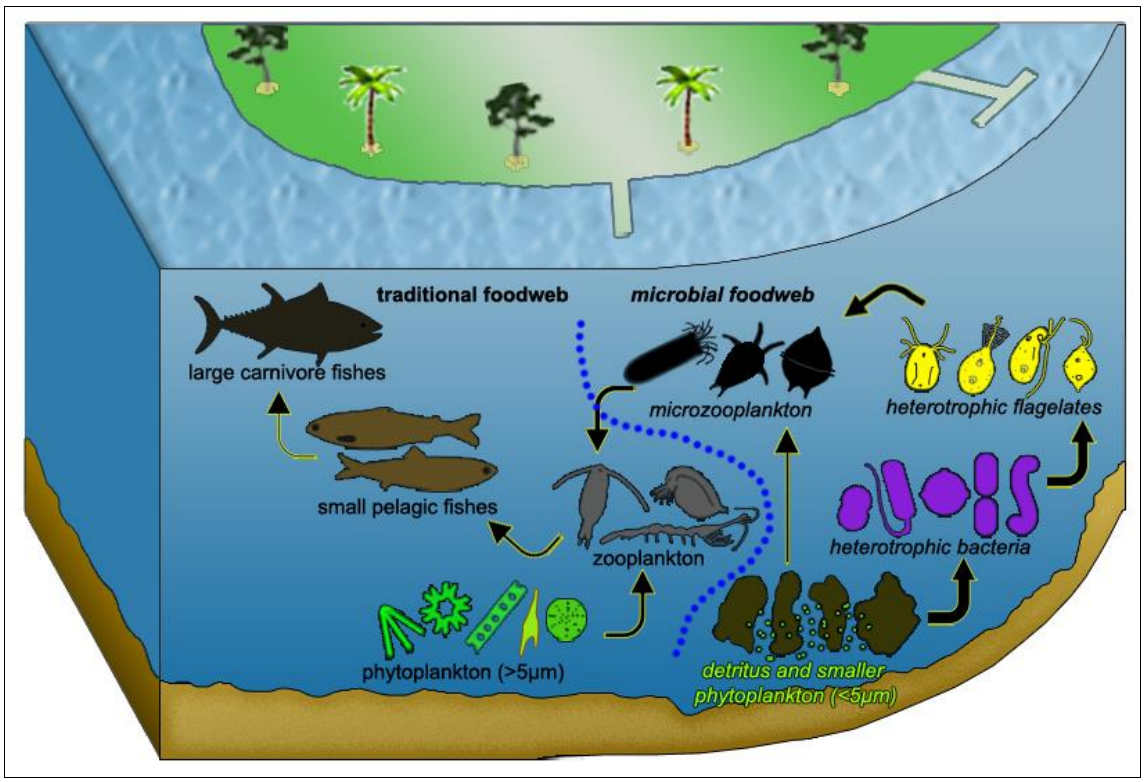

Figure 8 - Simplified sketch of foodweb structure in the lower reaches of the Kochi Backwaters shows energy transfer from phytoplankton and detritus to higher trophic levels. The thickness of arrows indicates relative quantity of energy transfer. The blue dotted line separates the traditional and microbial foodweb components. The dissolved organic carbon from all dead matter is utilized/ mineralized by the heterotrophic bacteria (excluded in the sketch). The sketch adopted from Jyothibabu et al., (2006) and redrawn to the present situation.

No	Source	Estuary	High SPM (mg/L)	Low SPM (mg/L)
1	Rao et a., 2011	Mandovi estuary	Jul (158)	May (3)
2	Rao et a., 2011	Zuari estuary	Jul (90)	Aug (2)
3	Anilkumar et al., 1998	Baypore estuary	Jul (1221)	Jan (62) - Feb (26)
4	Parvathi et al., 2013	Kochi Backwater	Jul (50.1 ± 10.6)	Dec (28.9 ± 9.4)
5	Kumar et al., 2006	Muthupet lagoon	Jul-Aug (1.65)	Nov (0.5)
6	Sarma et al., 2009; Acharyya et al., 2012	Godavari estuary	Jun-Sep (440 ± 220)	Dec-May (50 ± 30)
7	Kumari & Rao, 2010	Krishna estuary	Sep (58.4)	Feb (48.7)
8	Ray et al., 1984	Mahanadi estuary	Aug (261 ± 154)	Jan (2.8 ± 1.8)
9	Mukhopadhyay et al., 2006	Hooghly estuary	Jun-Sep (156.7)	Feb-May (32.5)
10	Kumar & Sarma, 2018	Major, medium and minor estuaries of India	Wet season August 2011	Dry season January 2012

Table 1 - The high and low values of total suspended particulate matter (SPM) reported in Indian estuaries during different months. It shows the highest SPM occurs during the monsoon periods when river runoff was in peak. SPM quantity in milligram per litre is given in parenthesis.

Table 2 - The mean hydrographical and biological variables (SD) during different seasons

Parameters	Southwest Monsoon	Northeast Monsoon	Pre-Southwest Monsoon
Salinity (PSU)	1.21 ± 0.78	14.41 ± 2.47	11.74 ± 1.78
PAR (µE m^{-2} s^{-1})	385 ± 22	464 ± 9	520 ± 21
Turbidity (NTU)	22.1 ± 12.5	7.9 ± 5.3	6.5 ± 5.1
Rainfall (mm h^{-1})	0.42 ± 0.007	0.09 ± 0.002	0.14 ± 0.003
Nitrate (µM L^{-1})	24 ± 3.2	6 ± 0.95	4 ± 0.87
Phosphate (µM L^{-1})	2.09 ± 0.27	1.15 ± 0.21	2.09 ± 0.21
Silicate (µM L^{-1})	74 ± 10.9	15 ± 4.18	23 ± 8.7
Abundance of Auto. (L^{-1})	1827 ± 1056	1254 ± 679	23963 ± 17142
Biomass of Auto. (µgC L^{-1})	8 ± 2.53	1 ± 0.44	16 ± 9.49
Volume of Auto. (μm^3)	43510 ± 3611	35245 ± 8655	20883 ± 2239
Abundance of Het. (L^{-1})	157 ± 81	299 ± 88	725 ± 184
Biomass of Het. (µgC L^{-1})	1.33 ± 0.5	3.19 ± 1.37	11.09 ± 3.39
Volume of Het. (μm^3)	125182 ± 19802	152844 ± 23758	201286 ± 11854
Abundance of Detritus (L^{-1})	5890 ± 1933	11064 ± 4990	26389 ± 4979
Volume of Detritus (mm^3 L^{-1})	0.32 ± 0.08	0.54 ± 0.14	0.47 ± 0.16

Table 3 - The seasonal mean abundance of micro--plankton in the downstream of the Kochi backwaters (Symbol representations: -- is absent, + is 1-100, ** is 101-1000, # is 1001-10000, ## is >10000).

No	Genus	Summer	Winter	Spring	No	Genus	Summer	Winter	Spring
1	*Actinastrum*	+	--	--	33	*Pseudo-nitzchia*	+	+	+
2	*Amphiprora*	+	+	--	34	*Rhizosolenia*	+	+	--
3	*Asterionella*	+	+	+	35	*Scenedesmus*	+	--	--
4	*Bacillaria*	+	--	--	36	*Selenastrum*	+	--	--
5	*Cerataulina*	+	+	--	37	*Skeletonema*	#	#	##
6	*Ceratium*	+	+	+	38	*Spirulina*	+	+	--
7	*Chaetoceros*	**	+	+	39	*Staurastrum*	**	--	+
8	*Coelastrum*	+	--	+	40	*Streptotheca*	--	+	--
9	*Corethron*	--	+	--	41	*Surirella*	+	+	**
10	*Coscinodiscus*	+	+	--	42	*Synedra*	--	--	+
11	Cyanobacteria	**	+	**	43	*Thalassionema*	--	+	+
12	*Dictyocha*	--	+	--	44	*Thalassiosira*	**	**	#
13	*Dinobryon*	+	--	--	45	Unid.Auto	**	**	**
14	*Dinophysis*	--	+	--	46	*Volvox*	+	--	--
15	*Ditylum*	+	+	--	47	*Acanthometron*	+	+	+
16	*Eucampia*	+	+	--	48	Bivalve larvae	+	**	+
17	*Eunotia*	#	--	+	49	Copepod	+	+	**
18	*Fragilaria*	+	+	+	50	*Favella*	+	--	+
19	*Guinardia*	--	+	--	51	Foraminifera	+	--	--
20	*Gyrosigma*	+	--	+	52	*Gymnodinium*	+	--	**
21	*Haslea*	--	+	--	53	*Gyrodinium*	+	--	--
22	*Leptocylindrus*	**	**	**	54	*Microdinium*	+	--	+
23	*Melosira*	+	+	--	55	Molluscan larvae	+	+	**
24	*Navicula*	+	--	--	56	Nauplius	+	**	**
25	*Nitzschia*	**	**	#	57	*Noctiluca*	+	--	--
26	*Odontella*	**	+	--	58	*Polykrikos*	+	--	--
27	*Oscillatoria*	+	--	--	59	*Protoperidinium*	+	**	**
28	*Pandorina*	+	--	--	60	Rotifer	**	+	**
29	*Paralia*	+	+	--	61	*Strombidium*	+	+	**
30	*Pediastrum*	+	+	**	62	*Tintinnopsis*	**	**	#
31	*Pinnularia*	--	--	+	63	Trochophore larvae	--	--	+
32	*Pleurosigma*	+	+	+	64	Unid.Hetero	**	+	**